HHS Public Access

Author manuscript

ACS Nano. Author manuscript; available in PMC 2018 April 25.

Published in final edited form as:

ACS Nano. 2017 April 25; 11(4): 4060–4066. doi:10.1021/acsnano.7b00725.

Fluorescence Resonance Energy Transfer-Based DNA Tetrahedron Nanotweezer for Highly Reliable Detection of Tumor-Related mRNA in Living Cells

Lei He[†], **Dan-Qing Lu**[†], **Hao Liang**[†], **Sitao Xie**[†], **Can Luo**[†], **Miaomiao Hu**[†], **Liujun Xu**[†], **Xiaobing Zhang**[†,*], and **Weihong Tan**[†,‡,*,ID]

[†]Molecular Science and Biomedicine Laboratory, State Key Laboratory of Chemo/Biosensing and Chemometrics, College of Chemistry and Chemical Engineering, College of Life Sciences, and Collaborative Innovation Center for Chemistry and Molecular Medicine, Hunan University, Changsha 410082, China

[‡]Department of Chemistry and Department of Physiology and Functional Genomics, Center for Research at the Bio/Nano Interface, Health Cancer Center, University of Florida, Gainesville, Florida 32611-7200, United States

Abstract

Accurate detection and imaging of tumor-related mRNA in living cells hold great promise for early cancer detection. However, currently, most probes designed to image intracellular mRNA confront intrinsic interferences arising from complex biological matrices and resulting in inevitable false-positive signals. To circumvent this problem, an intracellular DNA nanoprobe, termed DNA tetrahedron nanotweezer (DTNT), was developed to reliably image tumor-related mRNA in living cells based on the FRET (fluorescence resonance energy transfer) “off” to “on” signal readout mode. DTNT was self-assembled from four single-stranded DNAs. In the absence of target mRNA, the respectively labeled donor and acceptor fluorophores are separated, thus inducing low FRET efficiency. However, in the presence of target mRNA, DTNT alters its structure from the open to closed state, thus bringing the dual fluorophores into close proximity for high FRET efficiency. The DTNT exhibited high cellular permeability, fast response and excellent biocompatibility. Moreover, intracellular imaging experiments showed that DTNT could effectively distinguish cancer cells from normal cells and, moreover, distinguish among changes of mRNA expression levels in living cells. The DTNT nanoprobe also exhibits minimal effect of probe concentration, distribution and laser power as other ratiometric probe. More importantly, as a result of the FRET “off” to “on” signal readout mode, the DTNT nanoprobe almost entirely avoids false-positive signals due to intrinsic interferences, such as nuclease digestion, protein

[*]**Corresponding Authors**. xbzhang@hnu.edu.cn., tan@chem.ufl.edu.

ORCID

Weihong Tan: 0000-0002-8066-1524

ASSOCIATED CONTENT

Supporting Information

The Supporting Information is available free of charge on the ACS Publications website at DOI: 10.1021/acsnano.7b00725.

Supplementary spectral data (PDF)

The authors declare no competing financial interest.

binding and thermodynamic fluctuations in complex biological matrices. This design blueprint can be applied to the development of powerful DNA nanomachines for biomedical research and clinical early diagnosis.

Abstract

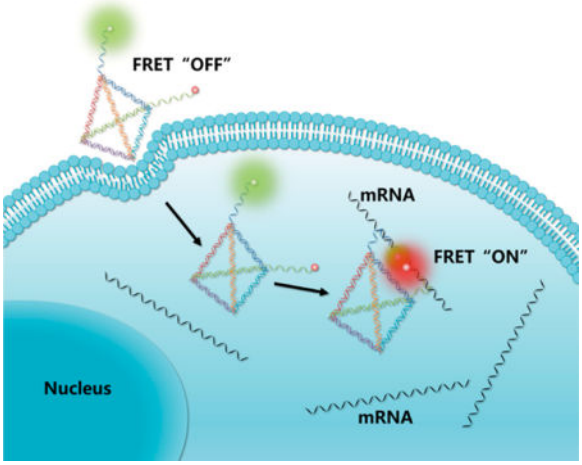

Identifying cancer at the cellular level at an early stage depends on the ability to distinguish abnormalities in gene expression in living cells.[1] The expression level of tumor-related mRNA can reveal significant information about tumor progression and prognosis.[2] Therefore, detection of endogenous tumor-related mRNA holds great promise for biological and disease studies.

Several well-known methods have provided insight into identifying and characterizing mRNA, including microarray analysis,[3–5] Northern blots,[6,7] and reverse transcription polymerase chain reaction (RT-PCR).[8,9] However, these approaches are not suitable for directly monitoring tumor-related mRNA at the cellular level, nor are they able to reveal transient spatiotemporal variations of RNA within a living cell. The resultant loss of important biological information has prompted the search for alternative approaches to mRNA detection in living cells. In this regard, nucleic acid-based fluorescence assays may be the most powerful and attractive techniques for detection of mRNA in living cells because of the high sensitivity, real-time and *in situ* monitoring capability and minimal harm to biological samples.[10,11] However, two pivotal issues need to be addressed when using nucleic acid-based fluorescent probes for the detection and imaging of tumor-related mRNA in living cells: effective delivery of probes into the cell and chemical interferences and thermodynamic fluctuations, that inevitably lead to high false-positive signals.[12–14] To address these challenges, approaches incorporating inorganic nanomaterials, such as gold nanoparticles and graphene, have been developed for cellular mRNA imaging.[15–19] These nanomaterials act as nanocarriers to deliver hydrophilic nucleic acids into the cells, and they also inhibit the enzymatic activity of some nucleases, resulting in enhanced stability of nucleic acids in biological environments.[20] Nonetheless, stability still remains a problem, and false-positive signals cannot be entirely avoided.[21] In addition, complex steps for the preparation and functionalization of these nanomaterials are commonly required.[22,23]

In recent years, DNA nanotechnology has been used for the rational assembly of many one-, two- and three-dimensional well-defined nanostructures, and some of them have been further applied in bioimaging, computation and drug delivery based on such advantages as excellent biocompatibility and nanoscale controllability.[24–26] For example, DNA tetrahedra, as recently emerged self-assembled DNA 3D nanomaterials, can be rapidly internalized through a caveolin-dependent pathway, remaining substantially intact within cells for at least 48 h.[27,28] This capability has significantly advanced their development in applications in sensor construction, drug delivery and molecular logic gates.[29–32] In fact, a few DNA tetrahedron-based probes have been assembled for sensing intracellular RNA.[29,33,34] Nevertheless, all of them are single-intensity-based sensing probes, which may lead to high false-positive signals from nuclease digestion, protein binding, or thermodynamic fluctuations.[21] Moreover, such sensing is compromised by the local distribution of probes and by drifts of light sources and detectors. These obstacles limit accurate detection and imaging of tumor-related mRNA in living cells.

In contrast, FRET-based probes, especially FRET “off” to “on”-based probes, can avoid false-positive signals and minimize the effects of system fluctuations in bioimaging.[35] So far, only a few DNA nanostructures have been used to image mRNA in living cells based on FRET. Unfortunately, all of them are traditional one- or two-dimensional DNA nanostructures.[36,37] Compared with 3D DNA nanostructures, these traditional one-or two-dimensional nanomaterials often show decreased cell permeability and much lower biostability, severely limiting their further development in bioimaging.[38] Therefore, it would be highly desirable, albeit challenging, to develop a 3D DNA nanoprobe that meets the requirements for accurate detection of tumor-related mRNA in living cells, including facile synthesis, high biocompatibility, self-delivery, and avoidance of false-positive signals caused by intrinsic chemical interferences and thermodynamic fluctuations.

Considering the excellent physical properties of 3D DNA nanostructures and the unparalleled advantages of FRET “off” to “on” signal readout in bioimaging, a ratiometric fluorescent nanoprobes, termed DNA tetrahedron nanotweezers (DTNTs), was developed to accurately image tumor-related mRNA in living cells. DTNTs are self-assembled from four customized single-stranded oligonucleotide strands. Scheme 1 illustrates the principle of DTNT for tumor-related mRNA detection. In the absence of target mRNA, the respectively labeled donor and acceptor fluorophores are separated, thus inducing low fluorescence resonance energy transfer (FRET) efficiency. However, in the presence of target mRNA, DTNT alters its structure from the open to closed state, thus bringing the dual fluorophores into close proximity and leading to high FRET efficiency. The FRET “off” to “on” signal readout mode can substantially avoid false-positive signals from complex biological matrices and provide a feasible platform for accurate detection. Therefore, we herein set up an excellent paradigm to rationally design self-assembled 3D DNA nanostructures for efficient and reliable imaging of tumor-related mRNA in living cells based on the FRET “off” to “on” signal readout mode.

RESULTS AND DISCUSSION

Preparation and Characterization of the DTNT Nanoprobe

As shown in Scheme 1, the DTNT nanoprobe was prepared by a simple annealing of four customized single-stranded oligonucleotide strands (S1, S2, S3 and S4, Table S1). Among the four strands, S2 and S3 were designed to have a target recognition site and were modified with Cy3 and Cy5, respectively. In the absence of a target, the donor fluorophore (Cy3) and receptor fluorophore (Cy5) were spatially separated. Thus, FRET was in the "off" state. However, the presence of a target resulted in target-induced configurational changes of the DTNT nanoprobe, shifting FRET from the "off" to "on" state. Successful formation of the DTNT nanoprobe was verified by use of AFM (Figure 1A) and 12.5% N-PAGE. As shown in Figure 1B, with the addition of strands from lane 1 to lane 4, a significant reduction of electrophoretic mobility could be clearly observed, which could be attributed to the increased molecular mass and more complex spatial construction. The results demonstrated that our DTNT nanoprobe had been successfully formed. By observing lane 5 (DTNT nanoprobe + target strand), no new band, except that of the DTNT nanoprobe, could be seen. Therefore, since our nanoprobe was demonstrated to have good target-binding ability, its response to the target strand was further investigated in the following fluorescence response experiments.

In Vitro Fluorescence Response of DTNT Nanoprobe

In order to investigate the behavior of our proposed DTNT nanoprobe, the fluorescence response of the nanoprobe was investigated. First, FRET signal changes of our DTNT nanoprobe were monitored in Tris-HCl buffer (20 mM Tris, 5 mM $MgCl_2$, pH = 8.0) upon changing the target concentration (0–100 nM). Figure 2A shows the fluorescence emission ratio of acceptor to donor (F_A/F_D) as a function of these target concentrations. In the absence of target DNA, the nanoprobe displayed only very low FRET signals. However, with the addition of target DNA, the fluorescence emission intensity of Cy3 (donor) at 565 nm decreased rapidly, whereas the fluorescence emission intensity of Cy5 (acceptor) at 662 nm increased. An almost 8.8-fold increase in F_A/F_D signal (from 0.13 to 1.15) was observed when the concentration of target DNA increased from 0 nM to 50 nM. This indicated that our nanoprobe could effectively recognize the target DNA and, in response, changed its structure from an open to a closed state, leading to a high FRET signal. Variation in FRET efficiency with target concentration was consistent with our postulated mechanism of the DTNT nanoprobe. Figure 2B describes-the relationship between changes in FRET signal and different concentrations of target DNA. The inset of Figure 2B shows a good linear correlation (R = 0.9927) from 0 to 20 nM with a limit of detection (LOD) of 0.33 nM based on the 3σ/slope rule.

Since it is important for probes to respond to their target rapidly, the response kinetics of DTNT toward target DNA was also tested by real-time monitoring of changes in fluorescence emission intensity of Cy3 at 565 nm and Cy5 at 662 nm, (Figure S1, Supporting Information (SI)). Results showed that the fluorescence of Cy3 decreases, while that of Cy5 rapidly increases with the addition of target DNA, suggesting that the nanoprobe can rapidly respond to the target. the F_A/F_D signal as a function of time showed the

hybridization between the targets and the probes was finished in 2 min. Collectively, the low detection limit and rapid target response kinetics indicate that this DTNT nanoprobe has the potential for further application in detecting tumor-related mRNA in living cells.

Ability of DTNT Nanoprobe to Avoid False-Positive Signals

DNA nanoprobes have been applied in complex biological systems. However, the greatest problem has always stemmed from intrinsic interferences that arise from such matrices, including false-positive signals. Therefore, in order to demonstrate the ability of DTNT nanoprobes to address this issue, the interaction of DTNT with Dnase I was first investigated. Dnase I is a powerful endonuclease capable of effectively degrading both single- and double-stranded DNA. When the samples were treated with 0.5 U/mL Dnase I, electrophoretic characterization (Figure 3A) showed that almost no degradation was observed and that our DTNT nanoprobe maintained its conformation at 1 h following treatment, which is consistent with previous studies indicating that the DNA tetrahedron could, to some degree, enhance nuclease resistance of the oligonucleotides on the nanostructure.[29] However, when the samples were treated with a higher concentration of Dnase I (5 U/mL), electrophoretic characterization showed that the DTNT nanoprobe was gradually digested and was almost completely digested at around 40 min. Nevertheless, as shown in Figure 3B, the F_A/F_D signal as a function of time showed no obvious changes, irrespective of treatment with low or high concentrations of Dnase I, strongly demonstrating that the DTNT nanoprobe could effectively resist false-positive signals caused by enzymatic degradation. Next, the effects of protein binding and thermodynamic fluctuations were studied by monitoring changes of the F_A/F_D signal. As shown in Figure S2, with an increase in BSA concentration, the fluorescence ratio (F_A/F_D) remained stable, and no false-positive signals were observed. Similar results were also observed with increasing temperature (Figure S3).

Benefiting from the FRET “off” to “on” signal readout mode, it is plausible that DTNTs have more robust ability to avoid false-positive signals compared to traditional molecular beacon-based DNA nanoprobes in complex biological matrices. In order to prove this, our DTNT nanoprobe (50 nM) was incubated with buffer and HL7702 cell lysates, respectively, and an existing DNA tetrahedron-based molecular beacon nanoprobe (50 nM) was chosen as the control.[34] As shown in Figure S4, the DNA tetrahedron-based molecular beacon nanoprobe exhibited minimal and stable fluorescence in buffer by the quenching of FAM by Dabcyl. Importantly, a gradually increasing false-positive signal was clearly detected with the extension of incubation time when the DNA tetrahedron-based molecular beacon nanoprobe was incubated in the cell lysates. In contrast, the FRET signal of our DTNT nanoprobe remained stable, and no false-positive signals were observed, neither in buffer nor in cell lysates. These results clearly demonstrated that our DTNT nanoprobe could resist false-positive signals and more accurately image targets of interest in complex biological samples.

Cytotoxicity Investigation of the DTNT Nanoprobe

Toxicity is always a vital factor for probes designed to image and monitor targets of interest in living cells. Therefore, in order to investigate the cytotoxicity of the DTNT nanoprobe, a

standard colorimetric MTT assay was performed on HepG2 cells (human liver hepatocellular carcinoma cell line). In this case, different concentrations of the DTNT nanoprobe were incubated with HepG2 cells for different times from 6 to 48 h. As shown in Figure S5, the DTNT nanoprobe exhibited no cytotoxicity or side effects in living cells. These results confirmed that the DTNT nanoprobe could potentially be used for the intracellular detection of specific mRNA.

Intracellular Imaging of the DTNT Nanoprobe

Having demonstrated its success in avoiding false-positive signals and excellent biocompatibility, the DTNT nanoprobe was further studied for its ability to image specific intracellular targets. As a target, we chose TK1 mRNA, which is associated with cell division and is proposed to be a marker for tumor growth.[39] Previous reports have shown that TK1 is overexpressed in HepG2 cells, but not HL7702 cells. HepG2 cells were thus chosen as the model target cells, and HL7702 cells were used as the negative control. First, the cellular uptake ability of the DTNT nanoprobe was investigated. We incubated HepG2 cells with the DTNT nanoprobe (50 nM) and a nude single-strand DNA probe (50 nM). As shown in Figure S6, in cells incubated with the nude single-strand DNA probe, only a very weak Cy3 fluorescence could be observed and there was almost no Cy5 FRET signal. This suggested that the nude ssDNA probe is not suitable for imaging intracellular mRNA, as a consequence of its poor permeability and low biostability. In contrast, we saw obvious Cy3 and Cy5 fluorescence in HepG2 cells when incubated with the DTNT nanoprobe. This result suggested that DTNT could perform excellent self-delivery without the help of transfection agents, a result which could, in turn, be attributed to its tetrahedral nanostructure. These results also show that DTNT could perform intracellular imaging of mRNAs in live cells. In fact, the fluorescence imaging data (Figure S7) showed that the FRET signals in HepG2 cells were gradually increased with incubation time up to 4 h, indicating that this time point should be used in subsequent experiments.

In order to investigate the specificity of the DTNT nanoprobe in living cells, we detected TK1 mRNA in a positive cell line (HepG2) and negative cell line (HL7702). As shown in Figure 4, obvious FRET signals for TK1 mRNA in HepG2 cells were observed, but almost no FRET signals were observed in HL7702 cells. These results showed that the DTNT nanoprobe could distinguish different cell lines with distinct mRNA expression levels. Because expression levels of mRNA in the same cancer cells can be different at different stages of tumorigenesis, the capability of the DTNT nanoprobe to detect the changes in mRNA expression levels is significant. It has been reported that tamoxifen can induce the down-regulation of TK1 mRNA expression and that β-estradiol can induce its upregulation.[40] To test this in our study, HepG2 cells were divided into three groups: an untreated control group, a group treated with β-estradiol to increase the TK1 mRNA expression, and a third group treated with tamoxifen to decrease it. Then DTNT (50 nM) was used to detect TK1 mRNA in HepG2 cells of the three groups, respectively. As shown in Figure 5, the higher FRET signals in the β-estradiol-treated cells and lower FRET signals in the tamoxifen-treated cells could be clearly observed compared with those in the untreated cells. These results indicated that the DTNT nanoprobe can detect changes in mRNA expression level in living cancer cells.

CONCLUSION

In summary, we have designed an intracellular DNA nanoprobes, termed DNA tetrahedron nanotweezers (DTNTs) through DNA molecular assembly for highly efficient and reliable detection of tumor-related mRNA in living cells. The DTNT nanoprobe exhibited many outstanding merits, such as facile synthesis and excellent biocompatibility. More importantly, compared to the prevailing strategy of molecular beacon-based biosensor construction, our DTNT nanoprobe showed its own remarkable advantages. First, the design of our DTNT nanoprobe could overcome the drawbacks of dual-fluorophore labeling on the same oligonucleotide and provide a simpler and more cost-effective option for efficient intracellular monitoring for targets of interest. Second, the DTNT nanoprobe showed excellent self-delivery capability. Third, based on its FRET “off” to “on” signal readout mode, the DTNT nanoprobe almost does not generate any false-positive signals caused by intrinsic biological interferences. Finally, ratiometric measurement can greatly minimize the effects of system fluctuations, which is very important for accurate imaging in living cells. Therefore, we herein have made a great attempt to rational design and build a self-assembled 3D DNA nanoconstruct for effective imaging of tumor-related mRNA in living cells based on the FRET “off” to “on” signal readout mode. The brilliant physical properties combined with the outstanding advantages of FRET “off” to “on” signal readout strongly suggest the potential of this DTNT nanoprobe for further *in vitro* and *in vivo* applications in biomedical research and clinical diagnostics.

EXPERIMENTAL SECTION

Chemicals and Materials

All DNA oligonucleotides (Table S1, Supporting Information) were purchased from Sangon Biotech Co., Ltd. (Shanghai, China). The oligonucleotides were purified by high-performance liquid chromatography (HPLC). Dnase I and bovine serum albumin (BSA) were purchased from Takara Biotechnology Co. Ltd. (Dalian, China). Tamoxifen and β-estradiol were purchased from Sigma-Aldrich Chemical Co. Ltd. (St. Louis, MO). Unless specified, all other reagents used in this work were of analytical grade, commercially purchased from Sinopharm Chemical Reagent Co., Ltd. (Shanghai, China), and used without further treatment. Human hepatocellular liver carcinoma cell line (HepG2) and human hepatocyte cell line (HL7702) were obtained from our lab and cultured in 1640 (GIBCO) medium with 10% fetal calf serum (FBS) and 1% penicillin-streptomycin (PS, 10 000 IU penicillin and 10 000 μg/mL streptomycin, Multicell).

Instruments

All solutions used in the experiments were prepared using ultrapure water (resistance >18 MΩ cm), which was obtained through a Millipore Milli-Q ultrapure water system (Billerica, MA, USA). All fluorescence measurements were carried out on a Fluoromax-4 (HORIBA Jobin Yvon Inc., Edison, NJ) spectrofluorometer with a temperature controller. The excitation wavelength was fixed at 525 nm with recording emission range of 545–750 nm. All excitation and emission bandwidths were set at 5 nm. The pH values of corresponding solutions were measured by a Mettler–Toledo Delta 320 pH meter. AFM characterization of

the sample was observed by Bruker Multimode V8 Scanning Probe Microscopy (USA). The confocal fluorescence imaging studies were performed on an FV1000 confocal laser-scanning microscope.

Preparation of DTNT Nanoprobe

DTNT nanoprobe was self-assembled according to previous reports with slight modifications.41 In brief, four customized single-stranded oligonucleotide strands were mixed with the equal molar ratio in TM buffer (20 mM Tris, 50 mM $MgCl_2$, pH = 8.0). The stock solutions, which have a final concentration of 2 μM, were heated to 95 °C for 5 min and then cooled to 4 °C within 1 min and kept in a buffer for future use.

Electrophoresis Characterization

Native polyacrylamide gel electrophoresis (N-PAGE) was applied to directly characterize the self-assembly formation of the DTNT nanoprobe. Typically, a gradual increase (from S1 to S4) in the number of different DNA strands was added to lanes 1–4, respectively. The mixed solutions were separated by 12.5% N-PAGE with 1× TBE/Mg^{2+} buffer at 110 V for 1 h and analyzed by a fluorescence image scanner (FLA-3000G; Fuji, Tokyo, Japan). To monitor nuclease digestion of DTNT nanoprobe, low and high concentrations of Dnase I were respectively added to a mixed solution containing 3 μM DTNT nanoprobe and incubated for different times (0, 10, 20, 30, 40, 50, 60 min) at room temperature. Then, 12 μL of the resultant nanoprobe solutions were mixed with 2 μL of loading buffer (6×), followed by 3% agarose gel electrophoresis running at 110 V for about 30 min in 1× TBE buffer and analyzed by a fluorescence image scanner.

Fluorescence Measurements

For detection of targets in buffer solution, different concentrations of synthetic DNA targets (0, 2, 5, 10, 15, 20, 25, 30, 40, 50, and100 nM) were added to 200 μL of Tris-HCl buffered solution (25 mM Tris with 5 mM $MgCl_2$, pH = 8.0) containing 50 nM DTNT nanoprobe, followed by incubation for 5 min at room temperature. The fluorescence spectra of the mixture were collected from 545 to 750 nm with 525 nm excitation in a 200 μL quartz cuvette. All experiments were repeated at least three times. To investigate the kinetics of the detection process, real-time monitoring of fluorescence intensity was also performed.

Cytotoxicity

Cytotoxicity of the DTNT nanoprobe was assessed with a standard MTT assay. HepG2 cells (1×10^5 cells/well) were cultured in 96-well microtiter plates and incubated at 37 °C in 5% CO_2 for 24 h to each 85% confluency, and then different concentrations of DTNT nanoprobe (0, 50, and 100 nM) were added to each well after the original medium was removed. HepG2 cells were incubated with DTNT nanoprobe for 6, 12, 24, and 48 h. Subsequently, the cells were washed with DPBS buffer three times, and 20 μL of 5 mg/mL MTT (thiazolyl blue tetrazolium bromide) was added to each well with incubation at 37 °C for 4 h. After DMSO was added, the absorbance was recorded at 490 nm using a multimode microplate.

Confocal Fluorescence Imaging

For cell imaging experiments, HepG2 and HL-7702 cell lines were grown in 1640 (GIBCO) medium with 10% fetal calf serum (FBS) and 1% penicillin-streptomycin with 5% CO_2 at 37 °C for 12 h. Next, cells were washed with DPBS buffer three times and incubated with DTNT nanoprobe (50 nM) in fresh 1640 medium at 37 °C for another 4 h. After washing with DPBS three times, confocal fluorescence imaging studies were performed on the FV1000 confocal laser-scanning microscope.

Supplementary Material

Refer to Web version on PubMed Central for supplementary material.

Acknowledgments

This work was supported by the Foundation for Innovative Research Groups of NSFC (Grant 21521063), National Natural Science Foundation of China (Grants 21325520, 21327009, J1210040, 21177036), and the Science and Technology Project of Hunan Province (2016RS2009, 2016WK2002). This work is also supported by the National Institutes of Health (GM079359 and CA133086).

References

1. Hanahan D, Weinberg RA. Angiogenesis in Cancer and Other Diseases. Cell. 2000; 100:57–70. [PubMed: 10647931]
2. Schwarzenbach H, Hoon DS, Pantel K. Cell-Free Nucleic Acids as Biomarkers in Cancer Patients. Nat. Rev. Cancer. 2011; 11:426–437. [PubMed: 21562580]
3. Brown PO, Botstein D. Exploring the New World of the Genome with DNA Microarrays. Nat. Genet. 1999; 21:33–37. [PubMed: 9915498]
4. Couzin J. Microarray Data Reproduced, But Some Concerns Remain. Science. 2006; 313:1559.
5. Chen JJ. Key Aspects of Analyzing Microarray Gene-Expression Data. Pharmacogenomics. 2007; 8:473–482. [PubMed: 17465711]
6. Alwine JC, Kemp DJ, Parker BA, Reiser J, Renart J, Stark GR, Wahl GM. Detection of Specific RNAs or Specific Fragments of DNA by Fractionation in Gels and Transfer to Diazobenzyloxymethyl Paper. Methods Enzymol. 1979; 68:220–242. [PubMed: 94421]
7. Pall GS, Codony-Servat C, Byrne J, Ritchie L, Hamilton A. Carbodiimide-Mediated Cross-Linking of RNA to Nylon Membranes Improves the Detection of siRNA, miRNA and piRNA by Northern Blot. Nucleic Acids Res. 2007; 35:e60. [PubMed: 17405769]
8. Nolan T, Hands RE, Bustin SA. Quantification of mRNA Using Real-Time RT-PCR. Nat. Protoc. 2006; 1:1559–1582. [PubMed: 17406449]
9. VanGuilder HD, Vrana KE, Freeman WM. Twenty-Five Years of Quantitative PCR for Gene Expression Analysis. BioTechniques. 2008; 44:619–626. [PubMed: 18474036]
10. Bratu DP, Cha BJ, Mhlanga MM, Kramer FR, Tyagi S. Visualizing the Distribution and Transport of mRNAs in Living Cells. Proc. Natl. Acad. Sci. U. S. A. 2003; 100:13308–13313. [PubMed: 14583593]
11. Medley CD, Drake TJ, Tomasini JM, Rogers RJ, Tan WH. Simultaneous Monitoring of the Expression of Multiple Genes Inside of Single Breast Carcinoma Cells. Anal. Chem. 2005; 77:4713–4718. [PubMed: 16053280]
12. Boussif O, Lezoualc'h F, Zanta MA, Mergny MD, Scherman D, Demeneix B, Behr JP. A Versatile Vector for Gene and Oligonucleotide Transfer into Cells in Culture and *in Vivo*: Polyethylenimine. Proc. Natl. Acad. Sci. U. S. A. 1995; 92:7297–7301. [PubMed: 7638184]
13. Chen AK, Behlke MA, Tsourkas A. Avoiding False-Positive Signals with Nuclease-Vulnerable Molecular Beacons in Single Living Cells. Nucleic Acids Res. 2007; 35:e105. [PubMed: 17702767]

14. Kim Y, Sohn D, Tan W. Molecular Beacons in Biomedical Detection and Clinical Diagnosis. Int. J. Clin. Exp. Pathol. 2008; 1:105–116. [PubMed: 18784800]
15. Song S, Liang Z, Zhang J, Wang L, Li G, Fan C. Gold-Nanoparticle-Based Multicolor Nanobeacons for Sequence-Specific DNA Analysis. Angew. Chem., Int. Ed. 2009; 48:8670–8674.
16. Pan W, Zhang T, Yang H, Diao W, Li N, Tang B. Multiplexed Detection and Imaging of Intracellular mRNAs Using a Four-Color Nanoprobe. Anal. Chem. 2013; 85:10581–10588. [PubMed: 24088027]
17. Wu Z, Liu GQ, Yang XL, Jiang JH. Electrostatic Nucleic Acid Nanoassembly Enables Hybridization Chain Reaction in Living Cells for Ultrasensitive mRNA Imaging. J. Am. Chem. Soc. 2015; 137:6829–6836. [PubMed: 25969953]
18. Zhao X, Xu L, Sun M, Ma W, Wu X, Kuang H, Wang L, Xu C. Gold-Quantum Dot Core–Satellite Assemblies for Lighting Up MicroRNA *in Vitro* and *in Vivo*. Small. 2016; 12:4662–4668. [PubMed: 26849492]
19. Li L, Feng J, Liu HY, Li QL, Tong LL, Tang B. Two-Color Imaging of MicroRNA with Enzyme-Free Signal Amplification via Hybridization Chain Reactions in Living Cells. Chemical Science. 2016; 7:1940–1945.
20. Jayagopal A, Halfpenny KC, Perez JW, Wright DW. Hairpin DNA-functionalized Gold Colloids for the Imaging of mRNA in Live Cells. J. Am. Chem. Soc. 2010; 132:9789–9796. [PubMed: 20586450]
21. Yang Y, Huang J, Yang X, Quan K, Wang H, Ying L, Xie N, Ou M, Wang K. FRET Nanoflares for Intracellular mRNA Detection: Avoiding False Positive Signals and Minimizing Effects of System Fluctuations. J. Am. Chem. Soc. 2015; 137:8340–8343. [PubMed: 26110466]
22. Zhang PH, He ZM, Chen W, Chen JN, Zhao JJ, Zhu XN, Li CZ, Min QH, Zhu JJ. *In Situ* Amplification of Intracellular MicroRNA with MNAzyme Nanodevices for Multiplexed Imaging, Logic Operation, and Controlled Drug Release. ACS Nano. 2015; 9:789–798. [PubMed: 25525669]
23. He X, Zeng T, Li Z, Wang G, Ma N. Catalytic Molecular Imaging of MicroRNA in Living Cells by DNA-Programmed Nanoparticle Disassembly. Angew. Chem. 2016; 128:3125–3128.
24. Hu R, Zhang X, Zhao Z, Zhu G, Chen T, Fu T, Tan W. DNA Nanoflowers for Multiplexed Cellular Imaging and Traceable Targeted Drug Delivery. Angew. Chem., Int. Ed. 2014; 53:5821–5826.
25. You M, Zhu G, Chen T, Donovan MJ, Tan W. Programmable and Multiparameter DNA-Based Logic Platform for Cancer Recognition and Targeted Therapy. J. Am. Chem. Soc. 2015; 137:667–674. [PubMed: 25361164]
26. Li J, Zheng C, Cansiz S, Wu C, Xu J, Cui C, Liu Y, Hou W, Wang Y, Zhang L, Teng IT, Yang HH, Tan W. Self-Assembly of DNA Nanohydrogels with Controllable Size and Stimuli-Responsive Property for Targeted Gene Regulation Therapy. J. Am. Chem. Soc. 2015; 137:1412–1415. [PubMed: 25581100]
27. Walsh AS, Yin H, Erben CM, Wood MJ, Turberfield AJ. DNA Cage Delivery to Mammalian Cells. ACS Nano. 2011; 5:5427–5432. [PubMed: 21696187]
28. Liang L, Li J, Li Q, Huang Q, Shi J, Yan H, Fan C. Single-Particle Tracking and Modulation of Cell Entry Pathways of a Tetrahedral DNA Nanostructure in Live Cells. Angew. Chem., Int. Ed. 2014; 53:7745–7750.
29. Tay CY, Yuan L, Leong DT. Nature-Inspired DNA Nanosensor for Real-Time in Situ Detection of mRNA in Living Cells. ACS Nano. 2015; 9:5609–5617. [PubMed: 25906327]
30. Li J, Pei H, Zhu B, Liang L, Wei M, He Y, Chen N, Li D, Huang Q, Fan C. Self-Assembled Multivalent DNA Nanostructures for Noninvasive Intracellular Delivery of Immunostimulatory CpG Oligonucleotides. ACS Nano. 2011; 5:8783–8789. [PubMed: 21988181]
31. Lee H, Lytton-Jean AK, Chen Y, Love KT, Park AI, Karagiannis ED, Sehgal A, Querbes W, Zurenko CS, Jayaraman M, Peng CG, Charisse K, Borodovsky A, Manoharan M, Donahoe JS, Truelove J, Nahrendorf M, Langer R, Anderson DG. Molecularly Self-Assembled Nucleic Acid Nanoparticles for Targeted *in Vivo* siRNA Delivery. Nat. Nanotechnol. 2012; 7:389–393. [PubMed: 22659608]

32. Pei H, Liang L, Yao G, Li J, Huang Q, Fan C. Reconfigurable Three-Dimensional DNA Nanostructures for the Construction of Intracellular Logic Sensors. Angew. Chem., Int. Ed. 2012; 51:9020–9024.

33. Zhou W, Li D, Xiong C, Yuan R, Xiang Y. Multicolor-Encoded Reconfigurable DNA Nanostructures Enable Multiplexed Sensing of Intracellular MicroRNAs in Living Cells. ACS Appl. Mater. Interfaces. 2016; 8:13303–13308. [PubMed: 27195747]

34. Xie N, Huang J, Yang X, Yang Y, Quan K, Wang H, Ying L, Ou M, Wang K. A DNA Tetrahedron-Based Molecular Beacon for Tumor-Related mRNA Detection in Living Cells. Chem. Commun. 2016; 52:2346–2349.

35. Sapsford KE, Berti L, Medintz IL. Materials for Fluorescence Resonance Energy Transfer Analysis: Beyond Traditional Donor–Acceptor Combinations. Angew. Chem., Int. Ed. 2006; 45:4562–4589.

36. Santangelo PJ, Nix B, Tsourkas A, Bao G. Dual FRET Molecular Beacons for mRNA Detection in Living Cells. Nucleic Acids Res. 2004; 32:e57. [PubMed: 15084672]

37. Shigeto H, Nakatsuka K, Ikeda T, Hirota R, Kuroda A, Funabashi H. Continuous Monitoring of Specific mRNA Expression Responses with a Fluorescence Resonance Energy Transfer-Based DNA Nano-tweezer Technique That Does Not Require Gene Recombination. Anal. Chem. 2016; 88:7894–7898. [PubMed: 27458920]

38. Ozhalici-Unal H, Armitage BA. Fluorescent DNA Nanotags Based on a Self-Assembled DNA Tetrahedron. ACS Nano. 2009; 3:425–433. [PubMed: 19236081]

39. Brabender J, Danenberg KD, Metzger R, Schneider PM, Park J, Salonga D, Holscher AH, Danenberg PV. Epidermal Growth Factor Receptor and HER2-Neu mRNA Expression in Non-Small Cell Lung Cancer is Correlated with Survival. Clin. Cancer Res. 2001; 7:1850–1855. [PubMed: 11448895]

40. Li N, Chang C, Pan W, Tang BA. Multicolor Nanoprobe for Detection and Imaging of Tumor-Related mRNAs in Living Cells. Angew. Chem., Int. Ed. 2012; 51:7426–7430.

41. Goodman RP, Heilemann M, Doose S, Erben CM, Kapanidis AN, Turberfield AJ. Reconfigurable, Braced, Three- Dimensional DNA Nanostructures. Nat. Nanotechnol. 2008; 3:93–96. [PubMed: 18654468]

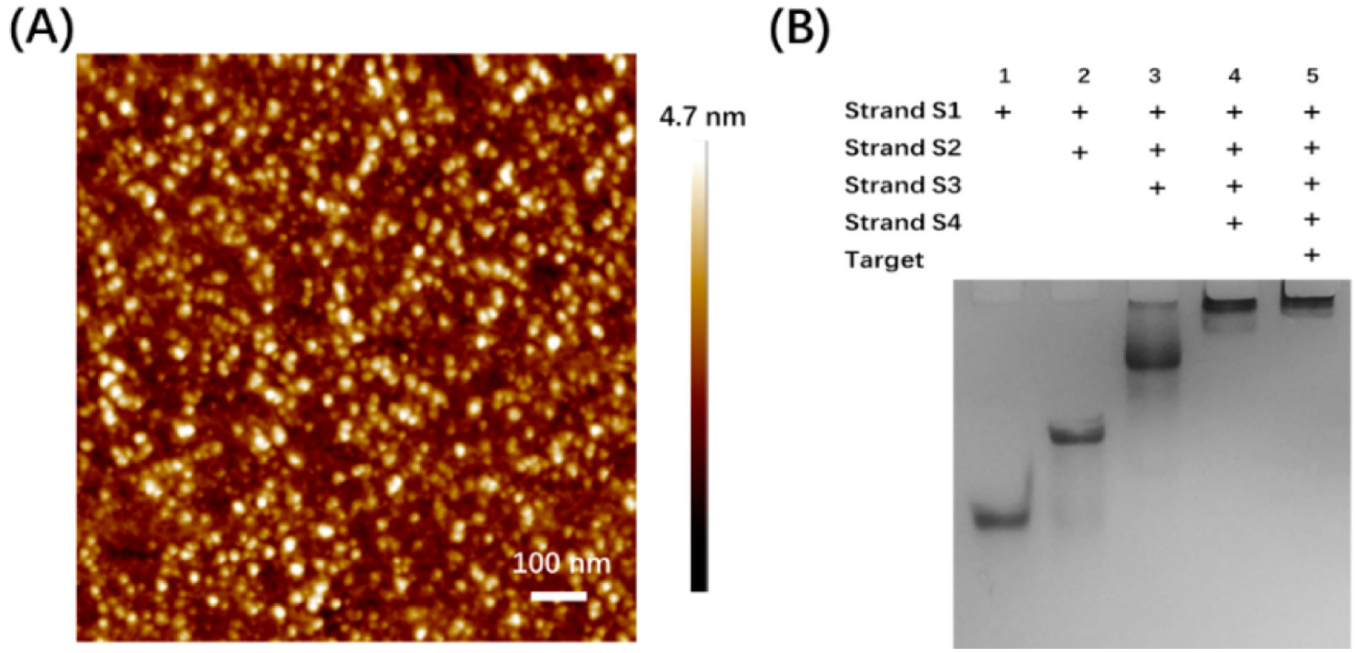

Figure 1.

(A) Characterization of DTNT by atomic force microscopy (AFM); Scale bars are 100 nm. (B) Analysis by 12.5% native PAGE. Lane 1 is strand S1; Lane 2 is strand S1 + strand S2; Lane 3 is strand S1 + strand S2 + strand S3; Lane 4 is strand S1 + strand S2 + strand S3 + strand S4; Lane 5 is strand S1 + strand S2 + strand S3 + strand S4 + target strand.

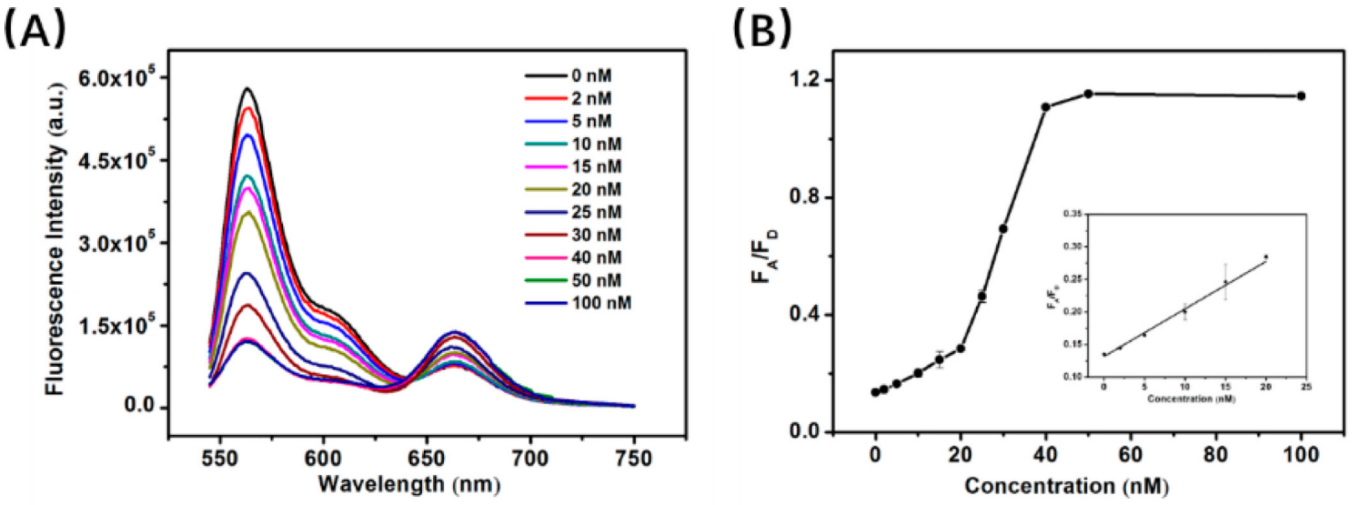

Figure 2.

(A) Fluorescence response in the presence of different concentrations of synthetic DNA targets, ranging from 0 to 100 nM. (B) The relationship between the fluorescence emission ratio of acceptor to donor (F_A/F_D) and target concentration. The inset shows the responses of the sensing system to target at low concentration.

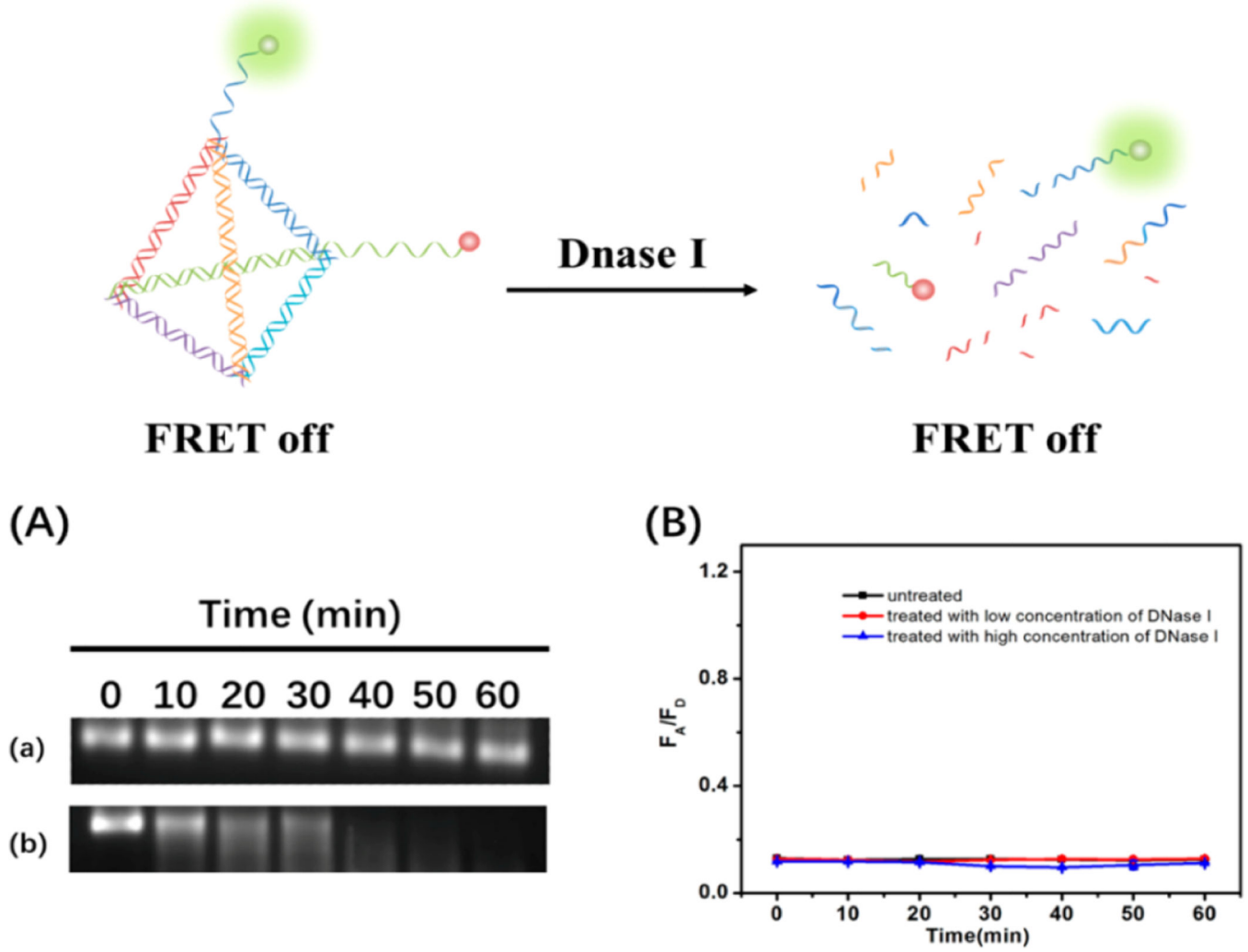

Figure 3.

(A) Electrophoresis characterization for the degradation of DTNT nanoprobe treated with (a) low concentration of Dnase I (0.5 U/mL) and (b) high concentration of Dnase I (5 U/mL). (B) Emission intensity ratio (F_A/F_D) as a function of time treated with different concentrations of Dnase I.

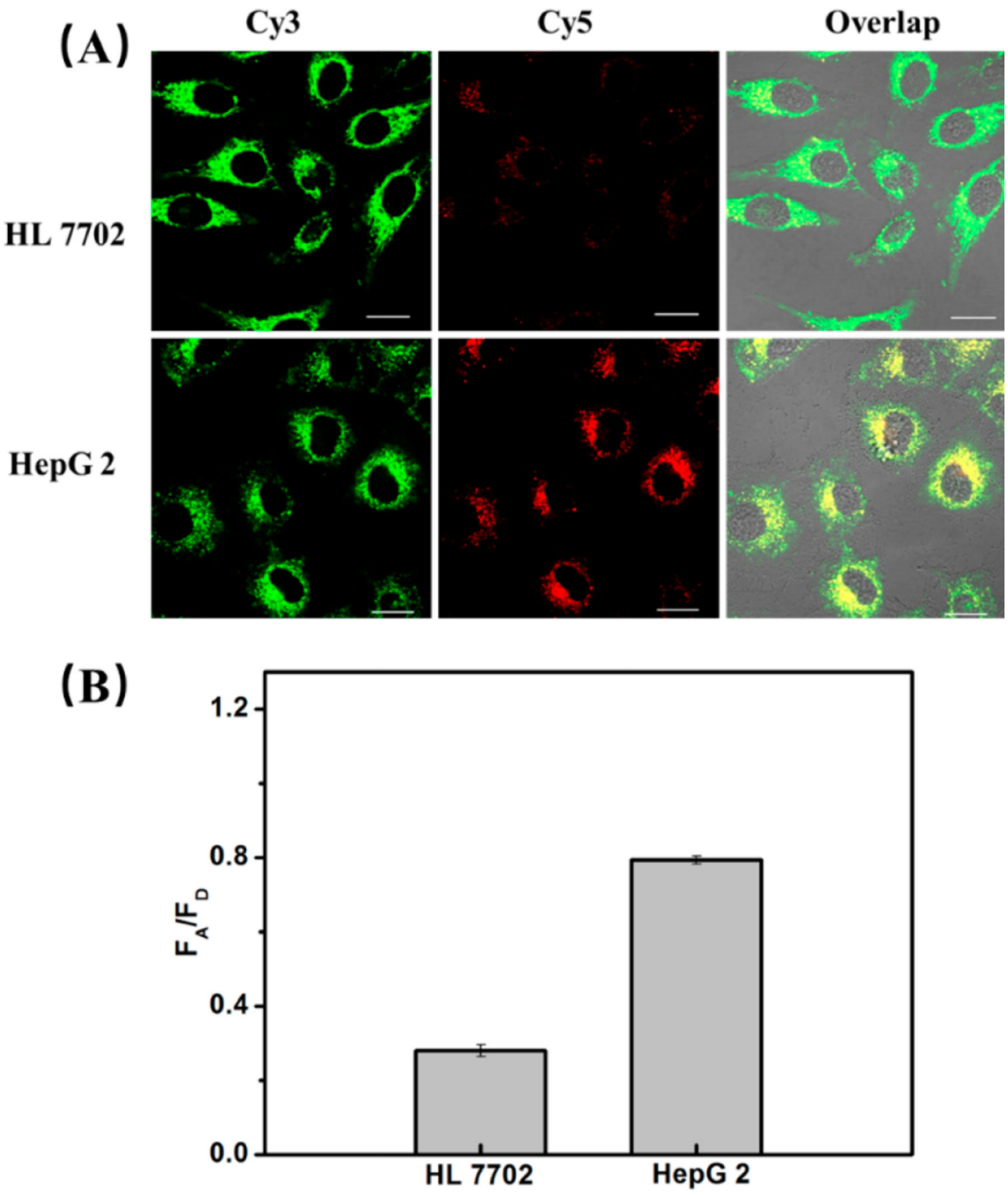

Figure 4.

(A) Fluorescence image of TK1 mRNA in HepG2 and HL7702 cells by DTNT nanoprobe. Scale bars are 20 μm. (B) Histogram of the relative fluorescence intensity (A/D) of the above two cell lines.

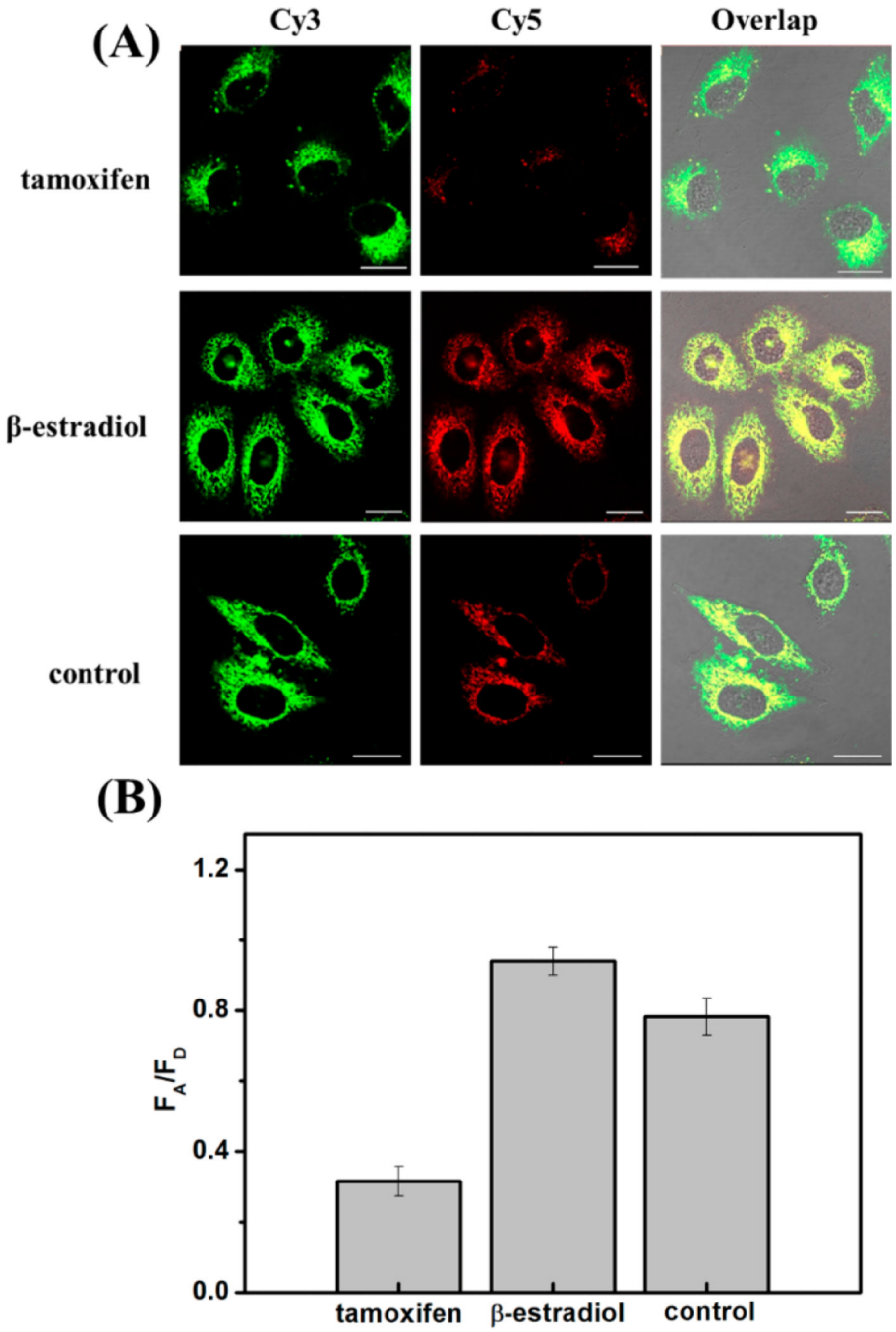

Figure 5.

(A) Fluorescence images of different expression levels of TK1 mRNA in HepG2 cells. Top panels are the tamoxifen-treated group, middle panels are the β-estradiol-treated group, and the bottom panels are the untreated group. Scale bars are 20 μm. (B) Histogram of the relative fluorescene intensity (A/D) of the above three groups.

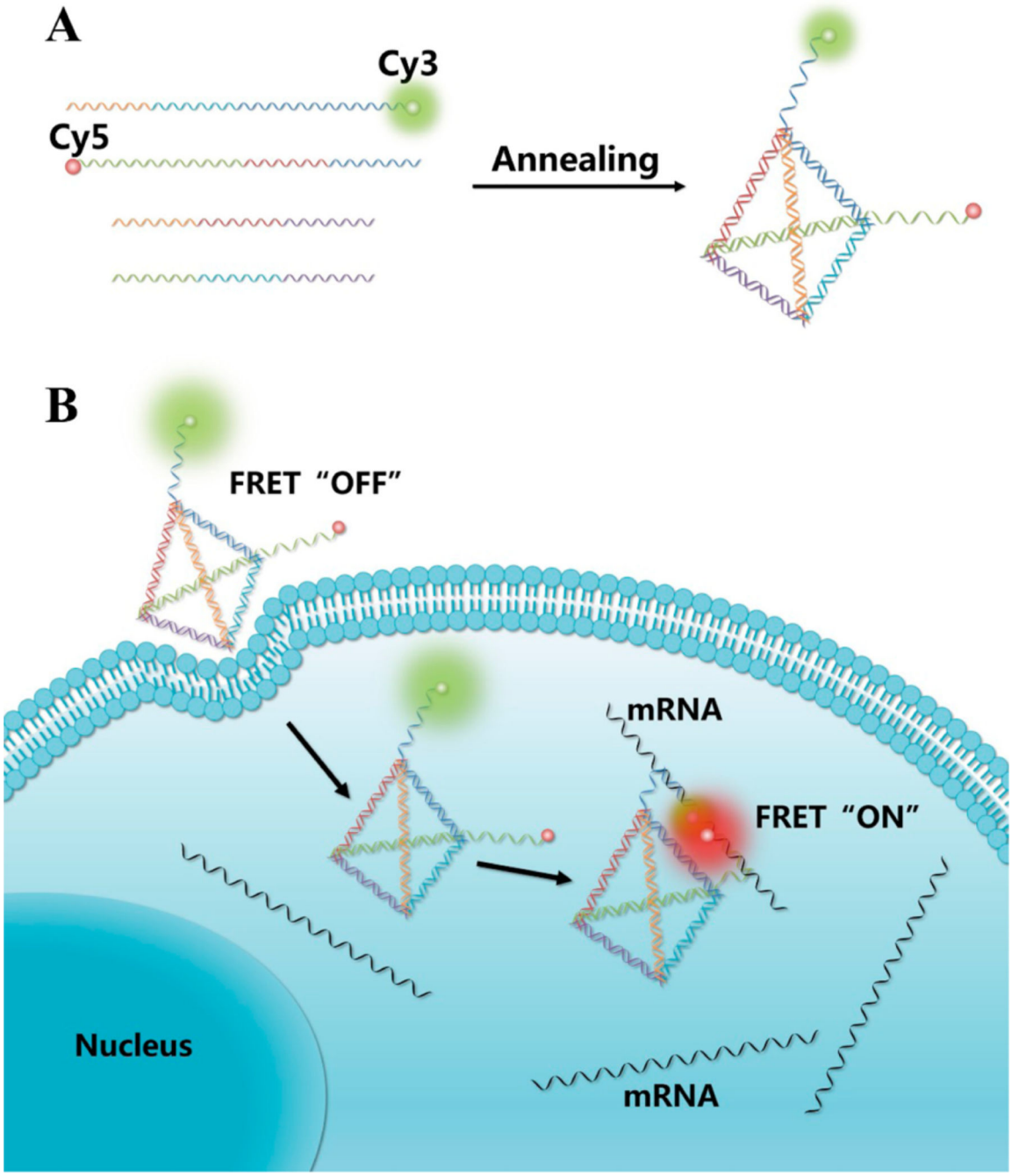

Scheme 1.

Synthesis (A) and Mechanism (B) of the DTNT Nanoprobe for Tumor-Related mRNA Detection in Living Cells